de Haas–van Alphen oscillations in the quasi-two-dimensional organic conductor κ-$(ET)_2Cu(NCS)_2$: The magnetic breakdown approach

V. M. Gvozdikov,[1,2] Yu. V. Pershin,[2,3] E. Steep,[2] A. G. M. Jansen,[2] and P. Wyder[2]
[1]*Department of Physics, Kharkov State University, 4 Svobody Sq.4, 61077, Kharkov, Ukraine*
[2]*Grenoble High Magnetic Field Laboratory, Max Planck Institut für Festkörperforschung and Centre National de la Recherche Scientifique, 25 Avenue des Martyres, B.P.166, F-38042 Grenoble Cedex 9, France*
[3]*B.I. Verkin Institute for Low Temperature Physics and Engineering, 47 Lenin Avenue, 61064, Kharkov, Ukraine*
(Received 29 January 2001; revised manuscript received 18 October 2001; published 27 March 2002)

We present both experimental data and an analytic theory for the de Haas–van Alphen (dHvA) effect in the two-dimensional organic single-crystal conductor κ-$(ET)_2Cu(NCS)_2$. We show that the magnetization oscillation pattern and the fast Fourier transform (FFT) spectrum of our measurements are well described theoretically within the coherent magnetic breakdown (MB) model for a two-dimensional Fermi surface consisting of two open sheets and closed pockets connected by magnetic breakdown centers. The spectrum of Landau quantized energy levels changes substantially due to the MB. Landau bands develop whose bandwidth and relative distance between them oscillate in inverse magnetic field. These oscillations explain the observed fine structure of the magnetization pattern at fields above the MB field with the occurrence of ''forbidden'' frequencies in the FFT spectrum.

DOI: 10.1103/PhysRevB.65.165102 PACS number(s): 71.18.+y, 75.20.En, 73.50.Jt, 74.70.Kn

I. INTRODUCTION

The quasi-two-dimensional (quasi-2D) ET salts form the largest organic superconductor family with unusual normal and superconducting properties[1–6] which come out of the layered structure as well as the specific shape of the Fermi surface. In this paper we report our experimental results on de Haas–van Alphen oscillations in the organic compound κ-$(ET)_2Cu(NCS)_2$ and give their theoretical explanation based on the coherent magnetic breakdown approach. The salt κ-$(ET)_2Cu(NCS)_2$ has a high superconducting transition temperature (about 10 K), and it is one of the most studied within the family of ET salts. It consists of alternating conducting layers composed of the BEDT-TTF molecules and insulating layers made of anions $Cu(NCS)_2$. de Haas–van Alphen (dHvA) and Shubnikov–de Haas (SdH) measurements of κ-$(ET)_2Cu(NCS)_2$ and other ET salts[7–15] done by different groups basically confirm the tight-binding-model-calculated Fermi surface (FS) shown in Fig. 1. The geometry of this FS implies a magnetic breakdown (MB) (i.e., magnetic-field-induced quantum tunneling) from the open sheet to the small closed α orbit (belonging to the neighboring Brillouin zone) and creating a new large closed β orbit which transverses three adjacent Brillouin zones.

The MB was introduced by Cohen and Falicov[16] as an important quantum complement to the semiclassical theory of metals of Lifshitz and Onsager. Further development of the theory of the MB was given in a number of works reviewed in Refs. 17 and 18 of which Stark and Falicov put emphasis on the stochastic aspects of the MB, whereas Kaganov and Slutskin discuss the coherent effects of MB. According to the coupled-network model of Pippard[19] and Falicov and Stachowiak,[20] which proved to be a good theoretical basis for description of MB in conventional metals, one has to observe different combinations of α and β frequencies (F_α and F_β) corresponding to different MB walks in Fig. 1. Surprisingly, the fast Fourier transform (FFT) of the magnetization oscillations displays some forbidden frequencies: $F_\beta - F_\alpha$ and $F_\beta - 2F_\alpha$, in particular. The term ''forbidden'' here stresses that the appropriate area of the Fermi surface is enclosed by a trajectory which cannot occur since it requires a sudden reversal of the electron movement in an external magnetic field. In the organic salt κ-$(ET)_2Cu(NCS)_2$ these frequencies have been observed in SdH (Refs. 9–11 and 21) as well as in dHvA experiments[7,8,13] and in the ac susceptibility of another ET salt α-$(ET)_2KHg(SCN)_4$.[14]

Although the forbidden frequencies were observed as early as 1982 in a dHvA study of coherent magnetic breakdown in magnesium,[22] their physical explanation remains yet an unsolved theoretical problem. The appearance of the forbidden frequencies in the SdH effect is more clear since they can be attributed (see Refs. 12 and 21, for example) to the so-called Stark interferometer.[23] The forbidden frequencies in the thermodynamic dHvA oscillations of κ-$(ET)_2Cu(NCS)_2$ have been studied analytically[24] and numerically.[12,25–29] All previous theories, except Refs. 25 and 26, interpret the forbidden frequencies as a result of the chemical potential oscillations in a 2D system with a fixed

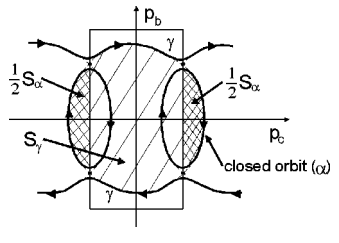

FIG. 1. The Fermi surface of κ-$(ET)_2Cu(NCS)_2$. Small α orbits are connected by the MB centers (solid circles) with two open sheets. The two major frequencies F_α and F_β of the dHvA oscillations are determined by the shaded areas S_α and $S_\beta = S_\alpha + S_\gamma$, respectively.

number of electrons (i.e., within the canonical ensemble scheme of calculations). The idea of the chemical potential oscillations in a 2D system with a fixed number of electrons was put forward by Peierls[30] and was developed later analytically by Vagner and co-workers[31,32] when 2D systems in high magnetic fields became an object of extensive experimental studies.

In view of the mathematical difficulties most of all theoretical works on the forbidden frequencies in dHvA studies have been made numerically either under the oversimplified two-band model approximation[12,28,29] or within the tight-binding Hofstadter approach.[25–27] In Ref. 25 an extensive numerical analysis of the dHvA oscillations in organic conductors κ-$(ET)_2Cu(NCS)_2$ and α-$(ET)_2KHg(SCN)_2$ was given within the canonical and grand canonical ensembles on the basis of first-principles calculations of the FS. The forbidden frequencies for both ensembles have been found but with a difference in the peak amplitudes.[25] The peaks of the permitted frequencies $F_\beta+F_\alpha$ and F_β are more suppressed in the canonical ensemble, while the forbidden frequency peaks $F_\beta-F_\alpha$ and $F_\beta-2F_\alpha$ are more suppressed in the grand canonical ensemble. Since the forbidden oscillations are present in both ensembles, the authors came to the conclusion that the chemical potential oscillations cannot be the origin of the forbidden frequencies in ET organic conductors. Rather they originate from the competition between the two Landau subbands (open sheets and closed orbits) at the Fermi surface. This conclusion is in agreement with the observation of the forbidden frequencies in dHvA oscillations of magnesium which is a conventional 3D metal, where the 2D mechanism of the chemical potential driven thermodynamic oscillations is irrelevant.[22]

Fotin and Ziman[24] extended the semiclassical theory by the inclusion of the magnetic breakdown within the mathematical scheme described in Kaganov and Slutskin's review.[18] They obtained forbidden frequencies as a result of the MB mixing of the open sheets and closed orbits in the canonical ensemble scheme at zero temperature and zero quasiparticle scattering range. Unfortunately, zero-temperature results are insufficient, for example, for the effective mass extraction from the experiment. To test the effective masses within the bands one has to have a theory valid for nonzero temperature since the effective masses are usually derived from the temperature dependence of the dHvA oscillation amplitudes.

Theoretically the dHvA amplitudes can be calculated after the energy spectrum is found. For the κ-$(ET)_2Cu(NCS)_2$ single crystal this implies a calculation of the energy spectrum in a MB chain of trajectories with the unit cell shown in Fig. 1. A model approach to the real energy spectrum of the ET salts was developed in Refs. 33 and 34. In these papers a real energy spectrum within the conducting planes was approximated by the model density of states (DOS) which is a combination of one-dimensional (open orbits) and two-dimensional (closed orbits) parts. The additional assumption was also made that the 1D DOS is independent of energy, giving the possibility to study the role of the specific ensemble (canonical or grand canonical) on the dHvA oscillations.

In this paper we calculate the energy spectrum for the MB configuration shown in Fig. 1. These calculations modify the theory for the dHvA effect in a chain of closed orbits coupled by coherent MB developed earlier by one of us[35] to the case of the Fermi surface configuration of the organic ET salts. We then apply the found energy spectrum for building up a theory for the dHvA oscillations in ET salts and compare our results with the recent experiment[13] of our group on dHvA in κ-$(ET)_2Cu(NCS)_2$. We will show that in the κ-$(ET)_2Cu(NCS)_2$ single crystals all observed deviations from the standard Lifshitz-Kosevich (LK) theory[36] (such as forbidden frequencies, in particular) can be explained by the MB-driven reorganization of the electronic energy spectrum with magnetic field. Physically this reorganization manifests itself as follows. At low magnetic fields, i.e., for field less than the magnetic breakdown field $B<B_0$, only small closed α orbits contribute to the quantum oscillations. For $B>B_0$ the MB-driven closed large β orbits appear which are connected by α orbits into a chain such that Landau bands may develop. Now both α and β orbits contribute into the dHvA oscillations and the FFT spectrum of these oscillations becomes more complicated because the frequencies F_α and F_β are incommensurate in general. The width and position of the Landau bands stemming from the β orbits oscillate with the frequency F_α because large β orbits are put together into a chain by dint of small closed α orbits which play the role of a quantum Stark interferometer (or effective MB center between β orbits). Therefore, effectively the frequency with which β Landau bands cross the Fermi level may be less (or more) than F_β with integer multiples of F_α. This means the appearance of forbidden frequencies in the FFT of the thermodynamic dHvA oscillations.

The above picture of dHvA oscillations differs from that in the standard LK approach valid for conventional metals. The principal difference is that in LK theory an external magnetic field does not change the energy spectrum of electrons and only determines the cross section of the Fermi surface which is independent of the magnetic field. On the contrary, in the coherent MB case the energy spectrum itself becomes a complex quasiperiodic function of the inverse magnetic field and strongly influences the dHvA oscillation pattern.

The paper is organized as follows. In Sec. II we present the details of the experimental magnetization oscillation measurements in single-crystal κ-$(ET)_2Cu(NCS)_2$. A sketch of the energy spectrum and the magnetization calculations is given in Sec. III. Section IV describes the experimental and theoretical results with their numerical comparison and discussion.

II. EXPERIMENT

We performed dHvA measurements on a κ-$(ET)_2Cu(NCS)_2$ single crystal. The sample was grown by electrochemical crystallization and had a weight of 0.8 mg. The experiments were performed in the hybrid magnet of the Grenoble High Magnetic Field Laboratory in the field range from 20 T to 27 T at temperatures between 0.4 K and 1.3 K provided by a ^{3}He cryostat. The magnetization was mea-

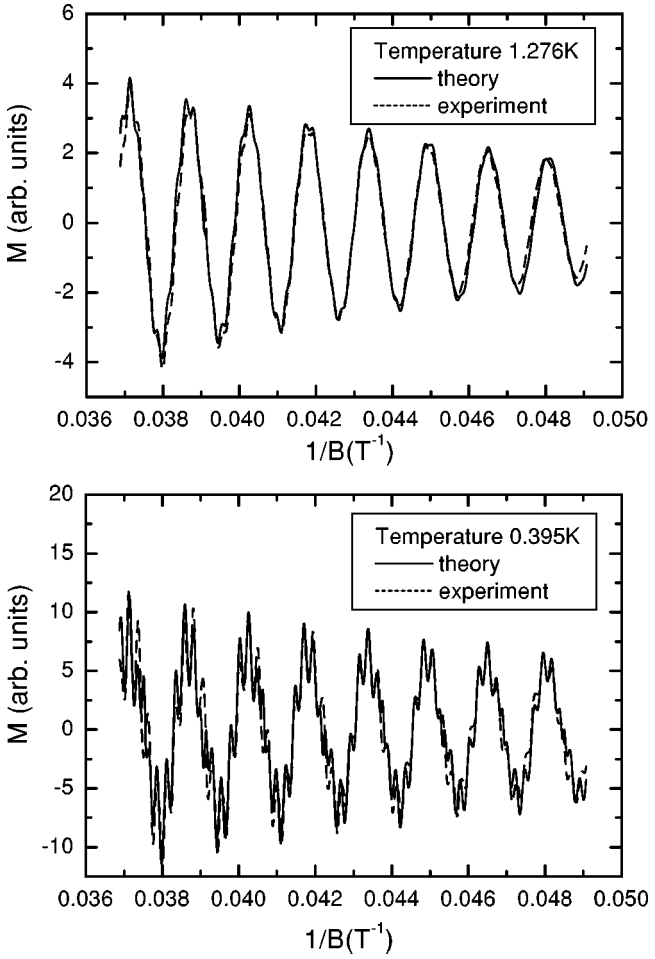

FIG. 2. Magnetization oscillation pattern as a function of inverse magnetic field for two different temperatures. Solid line: theory. Dashed line: experiment. The fit was done at the lowest temperature of 0.395 K. The fitting parameters are frequencies $F_\alpha = 639.5$ T and $F_\beta = 4166$ T, effective masses $m_\alpha = 3.3$ and $m_\beta = 7$, breakdown field $B_0 = 30$ T, Dingle temperatures $T_D^\alpha = 0.6$ K and $T_D^\beta = 0.45$ K, $\Gamma(B) = \Gamma_0 B$, $\Gamma_0 = 0.1$ T^{-1}, and g factor $= 1.6$ for α orbit and $g = 1.52$ for β orbit.

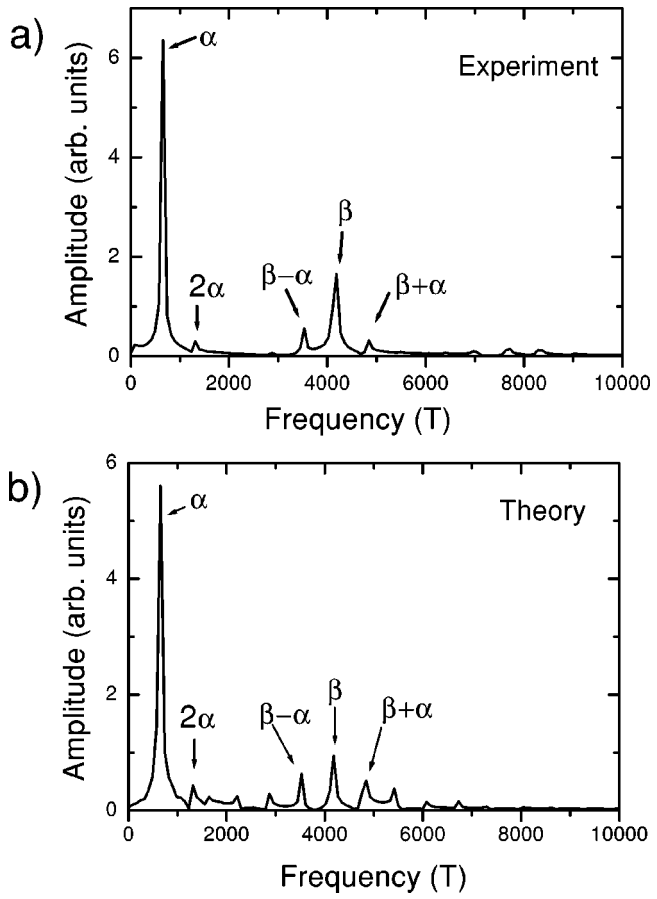

FIG. 3. The fast Fourier transform of the magnetization $M(1/B)$ at $T = 0.395$ K for the data in Fig. 2 for experiment (a) and theory (b). The "forbidden" peaks at frequencies $F_{\beta-\alpha}$ and $F_{2\beta-\alpha}$ are clearly seen.

sured using a capacitive cantilever torquemeter at an orientation $\Theta = 21°$. Here Θ is the angle between the magnetic field and the normal on the planes ($a^\star$ axis). The sample was rotated around the c axis.

The obtained oscillation patterns (at 0.395 K and 1.276 K) and FFT of the magnetization at 0.395 K are shown in Figs. 2 and 3. The forbidden frequencies are well distinguished. To be sure that these difference frequencies are not due to a nonlinear feedback of a finite torque on the torque signal (known as the torque interaction effect), we compensated the torque of the sample during the field sweep using a small coil which was glued on the cantilever beam. The absolute magnetization amplitude of the oscillations was estimated maximally as 5×10^{-5} T, which is too small to produce a nonlinear contribution to the signal from finite magnetization. Therefore also this effect of so-called magnetic interaction cannot explain the observation of anomalous difference frequencies in the dHvA signal.

III. ENERGY SPECTRUM AND THE de HAAS–van ALPHEN OSCILLATIONS

A. Energy spectrum

Now we turn to the theoretical description of the dHvA oscillations in κ-$(ET)_2Cu(NCS)_2$. The key issue is the energy spectrum. Since the FS shown in Fig. 1 is repeated infinitely in both directions of the p_c axis, we have a chain of closed α orbits coupled via MB centers (solid circles in Fig. 1) with two open sheets. Electrons move classically along the Fermi surface except in the close vicinity of the MB centers which act like a two-channel scattering center: they can either tunnel from one section of the FS to another with amplitude

$$\rho = \exp(-B_0/2B) \tag{1}$$

or may continue their classical motion along the same orbit with the amplitude τ. These quantum amplitudes are normalized by the condition $|\rho|^2 + |\tau|^2 = 1$, and B_0 is the magnetic breakdown field. Since the electron motion between neighboring MB centers is classical, the appropriate complete Feynman amplitude $e^{iS/\hbar}$ (S is the classical action) is given by the exponents $e^{i\varphi_{\alpha(\gamma)}}$ with the phases

$$\varphi_{\alpha(\gamma)}=\frac{c}{2e\hbar B}S_{\alpha(\gamma)}(E), \tag{2}$$

where S_α is the area inside the small closed α orbit in momentum space and S_γ stands for the area inside the two open sheets in the Brillouin zone (dashed area in Fig. 1). The relation between the phases $\varphi_{\alpha(\gamma)}$ and quantities $S_{\alpha(\gamma)}(E)$ is easy to understand. Consider, for example, a classical action along the upper γ segment of the open sheet in Fig. 1. It can be calculated as follows:

$$S=\int p_c dq_c=\frac{c}{eB}\int p_c dp_b=\frac{c}{2eB}S_\gamma(E). \tag{3}$$

Here p_b and p_c stand for the momentum projections on the b and c crystallographic axes; q_b and q_c are the corresponding coordinates. The quantity $e^{i\varphi_\gamma}\tau$ is the phase-coherent quantum amplitude of the following event: an electron starts at one side of the γ segment, then crosses the Brillouin zone, and finds itself beyond the MB center on the same open sheet of the FS (i.e., at the beginning of the γ segment in the neighboring Brillouin zone). The Feynman amplitude $e^{i\varphi_\gamma}\rho$ describes a similar event except that at the final stage the electron tunnels at the MB center to the closed α orbit. One can then easily write down a balance equation for the Feynman amplitudes in the neighboring cells of the Fermi surface. After that it becomes possible to build up a transfer matrix and to write down the corresponding dispersion relations which determine the energy spectrum of an electron at the FS shown in Fig. 1. The equations for large and small orbits can be decoupled and one of them (which yields the quantization rule for the large β orbit) reads[37]

$$|\tau_{eff}|\cos qL=\cos\left(\varphi_\gamma+\tilde{\varphi}_\alpha-\frac{\pi}{2}\right). \tag{4}$$

The quantities entering this equation are as follows: $\hbar q$ is the quasimomentum along the whole chain of orbits, L is the spatial period of the MB chain, $\tau_{eff}=\tau(1-\rho_{eff}e^{i\varphi_\alpha})$, where ρ_{eff} is the effective amplitude to tunnel from one open sheet to another through the small α orbit,

$$\rho_{eff}=\frac{\rho^2 e^{i\varphi_\alpha}}{1-\tau^2 e^{i2\varphi_\alpha}}, \tag{5}$$

and the quantity $\tilde{\varphi}_\alpha$ is related to the phase φ_α via the equation

$$\tilde{\varphi}_\alpha(E)=\arctan\left[\left(\frac{1+\tau^2}{1-\tau^2}\right)\tan\varphi_\alpha(E)\right]. \tag{6}$$

The effective MB amplitudes ρ_{eff} and τ_{eff} are normalized by the condition $|\rho_{eff}|^2+|\tau_{eff}|^2=1$. In the case of complete magnetic breakdown one has $\rho^2=1$, which also means that $\tau=\tau_{eff}=0$. From Eq. (6) we have in this case $\tilde{\varphi}_\alpha=\varphi_\alpha$ and after the substitution of this relation into Eq. (4) we arrive at the Lifshitz-Onsager quantization rule for the closed β orbit:

$$S_\beta(E)=\frac{2\pi e\hbar B}{c}(n+1). \tag{7}$$

Here $S_\beta=S_\gamma+S_\alpha$ is the area inside the closed β orbit composed of two α and two γ segments of the FS and n is a positive (large) integer since we work within the quasiclassical approach. Thus the closed β orbit is quantized according to the Lifshitz-Onsager quantization rule only under the condition of complete MB, $\rho^2=1$, when electrons rotate around this orbit with unit probability. In the case $\rho^2<1$ we can rewrite Eq. (4) in the form of a quantization rule:

$$S_\gamma(E)+\hat{S}_\alpha(E)=\frac{2\pi e\hbar B}{c}\left[(n+1)+\frac{(-1)^n}{\pi}\arcsin(|\tau_{eff}|\cos qL)\right], \tag{8}$$

where

$$\hat{S}_\alpha(E)=\frac{2e\hbar B}{c}\left\{\arctan\left[\left(\frac{1+\tau^2}{1-\tau^2}\right)\tan\left(\frac{cS_\alpha(E)}{2e\hbar B}\right)\right]\right\}. \tag{9}$$

We can see two differences between the quantization rules of Eqs. (7) and (8). First, Eq. (8) yields Landau bands rather than Landau levels where the last term in Eq. (8) describes the dispersion within the Landau bands. Second, Eq. (8) quantizes not the area inside the closed β orbit but the quantity $S_\gamma(E)+\hat{S}_\alpha(E)$ which is a ''quasiarea'' and differs from $S_\beta(E)$ because $\hat{S}_\alpha(E)\neq S_\alpha(E)$. In fact, this difference is very small: $\delta(E)=|\hat{S}_\alpha(E)-S_\alpha(E)|=0$ for $\rho^2=1$, $\delta(E)<0.03S_\alpha(E)$ for $\rho^2=0.9$, $\delta(E)<0.06S_\alpha(E)$ for $\rho^2=0.8$, and $\delta(E)<0.17S_\alpha(E)$ for $\rho^2=0.5$ and even for $\rho^2=0.1$ $\delta(E)<0.33S_\alpha(E)$. Thus only true closed orbits (which realize with the probability $\rho^2=1$) are quantized in the sense of the Lifshitz-Onsager quantization rule given by Eq. (7). For $\rho^2<1$ when multiple closed pathways are possible with different probabilities the resulting ''quasiarea'' is quantized by Eq. (8). This situation is like that which holds in superconductivity[38] where the magnetic flux is quantized in a thick hollow cylinder but another quantity, the fluxoid, is quantized in a thin one.

The Landau band energy spectrum is determined by Eq. (4). Generally, the Landau bands positions and their widths are quasiperiodic functions of the magnetic field as one can see from the equation

$$|\tau_{eff}|\leqslant\left|\cos\left[\varphi_\gamma(E)+\tilde{\varphi}_\alpha(E)-\frac{\pi}{2}\right]\right|. \tag{10}$$

The right-hand side of Eq. (10) is a combination of the two periodic functions with incommensurate periods which is the formal origin of the above quasiperiodicity. It is interesting to note in this connection that local aperiodicity of the MB energy spectrum was reported in a dHvA study of coherent MB in magnesium.[22] The quasiperiodicity of the energy spectrum in coherent MB systems is a general feature[18] which appears due to the incommensurability of two phases, $\varphi_\gamma(E)$ and $\tilde{\varphi}_\alpha(E)$ in our case. Nonetheless, near the Fermi

level, E_f, the energy spectrum is almost equidistant because $S_\alpha \ll S_\beta$ and we can put $\varphi_\alpha \simeq \varphi_\alpha(E_f)$ in Eq. (6). Then Eq. (8) yields the Landau bands whose width and positions are modulated periodically in inverse field with the periodicity of the function $|\rho_{eff}[\varphi_\alpha(1/B)]|$ [see Eq. (5)] which plays the role of an effective tunneling probability amplitude through the small α orbit. The function $\rho_{eff}[\varphi_\alpha(1/B)]$ can also be easily calculated as a result of the summation of all Feynman amplitudes with different numbers of revolutions around the small closed α orbit. We see, therefore, that Landau bands arise from the open sheets (γ sections) of the FS as a consequence of their correlations through small α orbits, which play the role of effective MB centers with effective tunneling probability $\rho_{eff}[\varphi_\alpha(1/B)]$. The small α orbits in their turn are coupled into a chain through open sheets of the FS but the appropriate equations are much more lengthy and will be published elsewhere. Physically it is clear that the correlations between α orbits are nonresonant (since they are mediated by the sections of the open orbits) and therefore less effective. As a first approximation we can take ρ_{eff} in this case as $\tilde{\rho}_{eff} \approx \rho \exp(i\varphi_\gamma)\rho$. The corresponding quantization rule for the α orbit in this case reads[35]

$$S_\alpha(E) = \frac{2\pi e\hbar B}{c}\left[(n+1/2) + \frac{(-1)^n}{\pi}\arcsin(|\tilde{\rho}_{eff}|\cos qL)\right]. \tag{11}$$

The second term in this equation describes the narrow and equidistant Landau bands whose width is proportional to $|\tilde{\rho}_{eff}| \approx \rho^2$ and vanish at $\rho = 0$.

Moreover, we would like to note that the MB energy spectrum considered above is a periodic function of the inverse magnetic field. This is important for what follows and makes the system in question different from conventional metals, where an external magnetic field only fixes the cross section of the FS but does not change the energy spectrum. This is the key point for the classical fermiology experiments, based on LK theory. We will show below that coherent MB brings fundamental corrections to LK theory.

B. dHvA oscillations

Knowledge of the energy spectrum allows us to calculate the magnetization M. We make these calculations for a 2D case within the grand canonical ensemble, i.e., for a fixed value of the chemical potential μ. This choice was made for the following reasons: (i) It was shown numerically in Ref. 25 that the oscillations of the chemical potential cannot be the origin of the forbidden frequencies. (ii) The recent analysis made in Ref. 39 revealed that only for low electron concentrations when $\hbar\Omega \approx \mu$ oscillations of μ with inverse magnetic field are important, where $\hbar\Omega$ is the Landau level spacing. In the case $\mu \gg \hbar\Omega$ the oscillations of the chemical potential are small and one can use the grand canonical ensemble as it holds in the standard LK theory. (iii) The inverse sawtooth shape of the magnetization was observed in ET salt,[2] which means a fixed chemical potential. Using the energy spectrum found above and making standard calculations one can present a magnetization in our case as a sum of contributions from α and β orbits with $S_\beta = S_\gamma + S_\alpha$ and

$$M = M_\alpha + M_\beta,$$

where

$$M_{\alpha(\beta)} = G_{\alpha(\beta)} \sum_{p=1}^{\infty} \frac{(-1)^p}{p} \sin\left(2\pi p \frac{F_{\alpha(\beta)}}{B}\right) \times R_D^{\alpha(\beta)}(p) R_T^{\alpha(\beta)}(p) R_S^{\alpha(\beta)}(p) I^{\alpha(\beta)}(p). \tag{12}$$

Here the following notation has been adopted: the constant

$$G_{\alpha(\beta)} = \frac{eS}{2\pi^2\hbar c}\frac{S_{\alpha(\beta)}}{m_{\alpha(\beta)}},$$

where S is the sample area. The indices α and β correspond, respectively, to small and large orbits. The frequencies F_α and F_β of the dHvA oscillations are due to the α and β orbits. They are related to the appropriate phases via equations $\varphi_{\alpha(\beta)} = \pi F_{\alpha(\beta)}/B$ and determined as follows: $F_\alpha = cS_\alpha(E_f)/2\pi e\hbar$ and $F_\beta = [S_\beta(E_f) + \delta_\alpha(E_f)]c/2\pi e\hbar$, where E_f is the Fermi energy. The quantity $\delta_\alpha(E_f) = \hat{S}_\alpha(E_f) - S_\alpha(E_f)$ describes a small deviation from the area enclosed by the β orbit as discussed above in the context of the quantization rules of Eq. (8). Four factors in Eq. (12) dampen the dHvA oscillation amplitudes. Among them there are three standard factors: (1) the temperature factor $R_T^{\alpha(\beta)}(p) = pX/\sinh(pX)$ which depends on mass and temperature through $X = am_{\alpha(\beta)}T/m_eB$, (2) the Dingle factor $R_D^{\alpha(\beta)}(p) = \exp(-pam_{\alpha(\beta)}T_D/m_eB)$ with Dingle temperature $T_D = \hbar/2\pi k_B\tau$ where τ is the lifetime of an electron on the appropriate cyclotron orbit, and (3) the spin reduction factor $R_S^{\alpha(\beta)}(p) = \cos[(\pi/2)pgm_{\alpha(\beta)}/m_e]$ where g is the so-called g factor. Another notation is as follows: $m_{\alpha(\beta)}$ are the effective electron masses while m_e stands for the mass of a free electron, the constant $a = 2\pi^2 m_e k_B/e\hbar = 14.69\ \mathrm{T\,K^{-1}}$.

The fourth type of reduction factor is due to the Landau bands caused by the coherent magnetic breakdown. For α and β orbits these factors are equal to $I^\alpha(p) = I_p(\rho^2)$ and $I^\beta(p)$ is given by

$$I^\beta(p) = (-1)^p \cos[2\pi p\gamma_{eff}] I_p(|\tau_{eff}|). \tag{13}$$

The quantity γ_{eff} is the effective phase shift of the Landau levels. It is a periodic function of the inverse field and determined by the relation $\gamma_{eff} = \pi^{-1}\tilde{\varphi}_\alpha(E_f)$ [see Eq. (6) for the definition of the function $\tilde{\varphi}_\alpha(E)$]. The reduction factor $I_p(\tau)$ standing in Eq. (13) is given by

$$I_p(\tau) = \frac{2}{\pi}\int_0^{\pi/2} dy \cos[2p\arcsin(\tau\cos y)]. \tag{14}$$

It dampens the dHvA oscillation amplitudes due to the finite Landau bandwidth. For sharp Landau levels ($\tau = 0$) this factor becomes unity $I_p(0) = 1$. This factor is also known in the dHvA oscillations of periodic coherent MB systems,[35] layered conductors,[40] and superconductors in the vortex-lattice

state.[41] Since the function $\cos[2p\arcsin(\tau\cos y)]$ can be rewritten in terms of the Chebyshev polynomials $T_{2p}(x)$ of the first kind as $T_{2p}[(1-\tau^2\cos^2 y)^{1/2}]$, the factor $I_p(\tau)$ is a polynomial of degree p in $\tau^2 \leqslant 1$ with the fixed values at the ends of a unit interval $I_p(0)=1$ and $I_p(1)=0$.[35] For the first harmonic $I_1(|\tau_{eff}|)=1-|\tau_{eff}|^2=|\rho_{eff}|^2 \propto \exp(-B_0/B)$. The latter means that the contribution of the β orbit into M grows with the field and oscillates in $1/B$ together with the effective tunneling probability through a small α orbit:

$$|\rho_{eff}|=\frac{\rho^2}{\sqrt{\rho^4+4(1-\rho^2)\sin^2(\pi F_\alpha/B)}}. \tag{15}$$

One can see from Eq. (15) that $|\rho_{eff}|$ equals unity every time the magnetic field satisfies the equation $\sin^2(\pi F_\alpha/B)=0$. For small tunneling probability $\rho \ll 1$ the oscillations of $|\rho_{eff}|$ are sharp and have the largest amplitude of the order of unity. Magneto-oscillations of the conductivity due to oscillations of the effective tunneling amplitude $|\rho_{eff}|$ in MB networks containing small closed orbits have been considered in Refs. 18 and 42. dHvA oscillations are also strongly affected by $|\gamma_{eff}|$ which determines the positions of the Landau bands and is a periodic function of $\varphi_\alpha(1/B)$ too.[35] Oscillations of the quantity γ_{eff} (Landau bands positions) with the period of α orbit in ET salts have been observed in Ref. 43. The coherence in periodic MB structures may be destroyed due to the small-angle electron scattering on phonons, dislocations, etc., which yield a small contribution into the Dingle factor, but should be taken into account in our case by the substitution $\varphi_\alpha \rightarrow \varphi_\alpha - i\Gamma(B)$.[18] The stochasticity parameter $\Gamma(B)$ controls a transition from the coherent MB regime $[\Gamma(B)=0]$ to the stochastic one $[\Gamma(B)\sim|\varphi_\alpha|]$. $\Gamma(B)$ is a phenomenological parameter whose dependence on B is unknown. Physically, $\Gamma(B)$ should increase with B since the probability to escape the small α orbit due to small-angle scattering increases when the trajectory radius ($\propto 1/B$) decreases.

IV. RESULTS AND DISCUSSION

A. dHvA oscillation pattern

The measurements of the dHvA oscillations were performed at different temperatures from 0.395 to 1.276 K. The oscillations patterns taken at lowest and highest temperatures are shown in Fig. 2. At low magnetic fields only small closed α orbits contribute to the magnetization oscillations with frequency $F_\alpha=639.5$ T. The fast Fourier transform of these oscillations yields peaks at F_α and $2F_\alpha$ only. At fields above the magnetic breakdown field B_0 (which we estimate as approximately 30 T) the FFT spectrum becomes much more richer. The FFT taken at the lowest temperature of 0.395 K is shown in Fig. 3(a). Except the two peaks due to the small orbits F_α and $2F_\alpha$ we see a rich structure of MB-driven peaks at F_β, $F_\beta \pm F_\alpha$, $F_\beta \pm 2F_\alpha$, $2F_\beta$, $2F_\beta \pm F_\alpha$, $2F_\beta \pm 2F_\alpha$ and peaks at $F_\beta+3F_\alpha$, $2F_\beta \pm 3F_\alpha$ which have the smallest amplitudes.

We made a fit of our theory [Eqs. (12)–(15)] to the experimental data at the lowest temperature of 0.395 K and find a good description of the experimental curves for increasing T up to 1.276 K without changing the fitting parameters (Fig. 2). These parameters were taken as follows: the small and large frequencies $F_\alpha=639.5$ T and $F_\beta=4166$ T, the effective masses are $m_\alpha=3.3m_e$ and $m_\beta=7m_e$, the breakdown field $B_0=30$ T, the Dingle temperatures for small and large orbits are $T_D^\alpha=0.6$ K and $T_D^\beta=0.45$ K, $\Gamma(B)=\Gamma_0 B$, $\Gamma_0=0.1$ T^{-1}, and g factor $=1.6$ for α orbit and $g=1.52$ for β orbit. We see, therefore, that our theory well fits the shape of the dHvA oscillations given by our experiments. What is important that the fit was made at the values of the parameters (frequencies, effective masses, g factors) taken from the literature on the organic superconductor κ-$(\mathrm{ET})_2\mathrm{Cu(NCS)}_2$ at the lowest temperature of 0.395 K and holds up to the highest experimental temperature of 1.276 K.

B. Forbidden frequencies

The experimental and theoretical FFT curves shown in Figs. 3(a) and 3(b) have similar shapes and harmonic content of forbidden frequencies. Both curves display clear peaks at frequencies F_α, F_β, and their second harmonics $2F_\alpha$, $2F_\beta$ as well as the satellites $F_\beta \pm F_\alpha$ of which the frequency $F_\beta - F_\alpha$ is classically prohibited. The appearance of the forbidden frequencies in our approach has a clear physical meaning. At low fields which are much less than the MB field, $B \ll B_0$, only oscillations due to the closed α orbits are resolved. When $B \gtrsim B_0$ and MB develops, the γ sections of the open sheets of the FS become connected through the α orbits and Landau bands appear whose dispersion is determined by Eq. (4). Because of the incommensurability of the α and β orbits, the energy spectrum is quasirandom (aperiodic). However, because of the big difference in the size of the α and β orbits, the width of the Landau bands and the separation between them oscillate with the frequency determined by the small α orbit. The quantization rule for these Landau bands is given by Eq. (8). Because of these oscillations, the effective frequency with which the Landau bands cross the Fermi level E_f may be either less or larger than F_β by an integer multiple of the frequency F_α.

The oscillating terms in M_β as follows from Eq. (12) appear due to the term

$$\sin\left(2\pi p\frac{F_\beta}{B}\right)\cos(2\pi p\gamma_{eff})I_p(|\tau_{eff}|^2). \tag{16}$$

The last two factors in Eq. (16) appear because of the Landau band position oscillation $[\cos(2\pi p\gamma_{eff})]$ and due to their bandwidth oscillation $[I_p(|\tau_{eff}|^2)]$ in the changing magnetic field. Now we can see how forbidden frequencies stem from this equation. Both of the above factors are even and periodic functions of the argument $\varphi_\alpha=\pi F_\beta/B$ and, therefore, can be presented as a series of the form

$$\cos(2\pi p\gamma_{eff})=\sum_{l=0}^{p} A_l^p \cos\left(2\pi\frac{F_\beta}{B}l\right), \tag{17}$$

$$I_p(|\tau_{eff}|^2)=\sum_{l=0}^{p} B_l^p \cos\left(2\pi\frac{F_\beta}{B}l\right). \tag{18}$$

The coefficients A_l^p can be obtained directly from Eqs. (17) and (6) with $\gamma_{eff}=\tilde{\varphi}_\alpha/\pi$ and $\tan\varphi_\alpha=(\sqrt{1-\cos^2\varphi_\alpha})/\cos\varphi_\alpha$. In the particular case $|\tau|\ll 1$, i.e., for the well-developed MB, $\cos(2\pi p\gamma_{eff})\approx\cos(2\pi pF_\alpha/B)$. The coefficients B_l^p one can write out too, by noting that $I_p(|\tau_{eff}|^2)$ is a polynomial of degree p in $|\tau_{eff}|^2$. For the first harmonics $p=1,2,3$, for example, we have

$$I_1=1-|\tau_{eff}|^2,$$

$$I_2=1-4|\tau_{eff}|^2+3|\tau_{eff}|^4,$$

$$I_3=1-9|\tau_{eff}|^2+18|\tau_{eff}|^4-10|\tau_{eff}|^6. \tag{19}$$

On the other hand, $|\tau_{eff}|^2=1-|\rho_{eff}|^2$ and the quantity $|\rho_{eff}|^2$, given by Eq. (15), can be written as a series

$$|\rho_{eff}|^2=A\sum_{n=0}^{\infty}\left(\frac{B}{2}\right)^n\sum_{k=0}^{\infty}C_n^k\cos\left(2\pi\frac{F_\alpha}{B}k\right), \tag{20}$$

where the coefficients A and B are given by $A=[\rho^2/(\rho^2-2)]^2$, $B=4(1-\rho^2)/(\rho^2-2)^2$, and $C_n^k=n!/(n-k)!k!$ is the Newtonian binomial coefficient. Putting Eqs. (16)–(18) into the series of Eq. (12), we have a sum of the form

$$\begin{aligned}M_\beta=&A_1\sin\left(2\pi\frac{F_\beta}{B}\right)+A_2\sin\left(2\pi\frac{F_\beta-F_\alpha}{B}\right)\\&+A_3\sin\left(2\pi\frac{F_\beta+F_\alpha}{B}\right)+A_4\sin\left(2\pi\frac{F_\beta-2F_\alpha}{B}\right)\\&+A_5\sin\left(2\pi\frac{F_\beta+2F_\alpha}{B}\right)+\cdots.\end{aligned} \tag{21}$$

We see, therefore, that the ''forbidden'' frequencies $F_\beta-F_\alpha$, $F_\beta-2F_\alpha$ as well as higher harmonics appear in the magnetization oscillation M_β as a result of the Landau bandwidth oscillations as well as due to the oscillations of their positions with the varying field. At high fields the small α orbits are coupled by the magnetic breakdown centers too, which results in the appearance of narrow Landau α bands. These bands only slightly decrease the magnetization amplitudes $M_\alpha(p)$ due to the factor $I^\alpha(p)=I_p(\rho^2)$ since the coupling of small orbits through the MB is nonresonant and yields no additional oscillations.

V. CONCLUSION

In conclusion, we put forward a coherent magnetic breakdown mechanism of dHvA oscillations in a quasi-2D organic conductor whose FS consists of two open sheets coupled by the MB. The proposed model fits rather well to our experimental data on the magnetization oscillations in κ-$(ET)_2Cu(NCS)_2$ single crystals. As most prominent result our theory explains the origin of the so-called forbidden frequencies in the FFT spectrum of the dHvA oscillations with a good theoretical fit to the experimental oscillation pattern within the whole range of investigated temperatures. This means that all information usually extracted from the dHvA oscillation pattern might be explained within the proposed coherent magnetic breakdown mechanism of the dHvA oscillations.

An interesting point in this connection is concerned with the standard method for the determination of the effective mass from a study of the temperature dependence of the FFT peak intensities for both permitted and forbidden frequencies. The temperature behavior of the harmonic amplitudes in the magnetization of Eq. (12) is due to the temperature reduction factor $R_T(p)$ as in LK theory. But on the other hand, because of the nonmonotonous behavior of the factor $I_p(|\tau_{eff}|)$ with magnetic field, the effective masses obtained at different values of the magnetic field may differ. A dependence of the effective masses on the magnetic field strength was observed in experiments on κ-$(ET)_2Cu(NCS)_2$ single crystals in a study of the temperature dependence of the FFT peak amplitudes of the magnetization pattern.[44] The change in effective mass may result from a contribution of the Landau bands because, roughly speaking, the effective mass of the electrons within the Landau bands is inversely proportional to their bandwidth which is a nonmonotonous function of the external magnetic field. On the contrary, the effective masses in LK theory are determined only by the cross sections of the Fermi surface which depend on the orientation of the magnetic field but not on the field strength. Once determined from the temperature factor $R_T(\rho)$, these masses should not depend on magnetic field in LK theory since the cross sections of the Fermi surface do not depend on the magnetic field intensity. But this is no longer the case for periodic MB systems. A detailed analysis of this effect will be considered separately in a forthcoming publication.

Our consideration of periodic magnetic breakdown orbits is relevant to the quasi-2D conductors whose FS consists of 1D open trajectories and 2D closed orbits connected by the magnetic breakdown. Apart from the interest of the magnetic breakdown phenomenon for the ET salts, the phenomenon may be of importance for the magnetoquantum oscillations in the newly artificially made 2D lateral superlattices.[45] Many unusual features have been observed in Shubnikov–de Haas measurements made on the ET salts[2,46,47] for which the magnetic breakdown approach developed in this paper might be useful for better insight into the Shubnikov–de Haas effect in layered organic superconductors.

We greatly acknowledge stimulating discussions with I. D. Vagner, T. Maniv, A. M. Dyugaev, P. Grigoriev, M. V. Kartsovnik, and W. Biberacher.

[1] J. Wosnitza, S. Wanka, J. Hagel, J. S. Qualls, J. S. Brooks, N. Harrison, E. Balthes, D. Schwetzer, J. A. Schlueter, U. Geiser, J. Mohtasham, R. W. Winter, and G. L. Gard, Physica B **294-295**, 442 (2001).

[2] J. Wosnitza, S. Wanka, J. Hagel, E. Balthes, N. Harrison, J. A. Schlueter, A. M. Kini, U. Geiser, J. Mohtasham, R. W. Winter, and G. L. Gard, Phys. Rev. B **61**, 7383 (2000).

[3] T. G. Togonidze, M. V. Kartsovnik, J. A. A. J. Perenboom, N. D.

Kushch, and H. Koboyashi, Physica B **294-295**, 435 (2001).
[4] J. S. Brooks, L. Balicas, M. Tokumoto, T. Terashima, Y. Echizen, and T. Takabatake, Physica B **294-295**, 408 (2001).
[5] J. A. Symington, J. Singleton, N. Clayton, J. Schlueter, M. Kurmoo, and P. Day, Physica B **294-295**, 439 (2001).
[6] N. J. Clayton, H. Ito, S. M. Hayden, P. J. Meeson, and M. Springfield, Phys. Rev. B **65**, 064515 (2002).
[7] F. A. Meyer, E. Steep, W. Biberacher, P. Christ, A. Lerf, A. G. M. Jansen, W. Joss, and P. Wyder, Europhys. Lett. **32**, 681 (1995).
[8] S. Uji, M. Chaparala, S. Hill, P. S. Sandhu, J. Qualls, L. Seger, and J. S. Brooks, Synth. Met. **85**, 1573 (1997).
[9] C. P. Heidmann, H. Mueller, W. Biberacher, K. Neumaier, C. Probst, K. Andres, A. G. M. Jansen, and W. Joss, Synth. Met. **41-43**, 2029 (1991).
[10] T. Sasaki, H. Sato, and N. Toyota, Solid State Commun. **76**, 507 (1990).
[11] J. Caulfield, J. Singleton, F. L. Pratt, M. Doporto, W. Lubczynski, W. Hayes, M. Kurmoo, P. Day, P. T. J. Hendriks, and J. A. A. J. Perenboom, Synth. Met. **61**, 63 (1993).
[12] N. Harrison, J. Caulfield, J. Singleton, P. H. P. Reinders, F. Herlach, W. Hayes, M. Kurmoo, and P. Day, J. Phys.: Condens. Matter **8**, 5415 (1996).
[13] E. Steep, L. H. Nguyen, W. Biberacher, H. Muller, A. G. M. Jansen, and P. Wyder, Physica B **259-261**, 1079 (1999).
[14] M. M. Honold, N. Harrison, M. S. Nam, J. Singleton, C. H. Mielke, M. Kurmoo, and P. Day, Phys. Rev. B **58**, 7560 (1998).
[15] M. Schiller, W. Schmidt, E. Balthes, D. Schweitzer, H.-J. Koo, M. H. Whangbo, I. Heinen, T. Klausa, P. Kircher, and W. Strunz, Europhys. Lett. **51**, 82 (2000).
[16] M. H. Cohen and L. M. Falicov, Phys. Rev. Lett. **7**, 231 (1961).
[17] R. W. Stark and L. M. Falicov, Prog. Low Temp. Phys. **5**, 235 (1967).
[18] M. I. Kaganov and A. A. Slutskin, Phys. Rep. **98**, 189 (1983).
[19] A. B. Pippard, Proc. R. Soc. London, Ser. A **287**, 165 (1965).
[20] L. M. Falicov and Henryk Stachowiak, Phys. Rev. **147**, 505 (1966).
[21] M. V. Kartsovnik, G. Yu. Logvenov, T. Ishiguro, W. Biberacher, H. Anzai, and N. D. Kushch, Phys. Rev. Lett. **77**, 2530 (1996).
[22] J. W. Eddy, Jr. and R. W. Stark, Phys. Rev. Lett. **48**, 275 (1982).
[23] R. W. Stark and R. Reifenberger, J. Low Temp. Phys. **26**, 763 (1977).
[24] J. Y. Fotin and T. Ziman, Phys. Rev. Lett. **80**, 3117 (1998).
[25] J. H. Kim, S. Y. Han, and J. S. Brooks, Phys. Rev. B **60**, 3213 (1999).
[26] S. Y. Han, J. S. Brooks, and J. H. Kim, Phys. Rev. Lett. **85**, 1500 (2000).
[27] K. Mashida, K. Kishigi, and Y. Hori, Phys. Rev. B **51**, 8946 (1995).
[28] M. Nakano, J. Phys. Soc. Jpn. **66**, 19 (1997).
[29] A. S. Alexandrov and A. M. Bratkovsky, Phys. Rev. Lett. **76**, 1308 (1986).
[30] R. E. Peierls, Z. Phys. **81**, 186 (1933).
[31] I. D. Vagner, T. Maniv, and E. Ehrenfreund, Phys. Rev. Lett. **51**, 1700 (1983); K. Jauregui, V. I. Marchenko, and I. D. Vagner, Phys. Rev. B **41**, 12 922 (1990).
[32] M. A. Itskovsky, T. Maniv, and I. D. Vagner, Z. Phys. B: Condens. Matter **101**, 13 (1996).
[33] N. Harrison, R. Bogaerts, P. Reinders, J. Singleton, S. J. Blundell, and F. Herlach, Phys. Rev. B **54**, 9977 (1996).
[34] P. Grigoriev, Zh. Exp. Teor. Fiz. **119**, 1257 (2001) [JETP **92**, 1090 (2001)].
[35] V. M. Gvozdikov, Sov. J. Low Temp. Phys. **12**, 399 (1986).
[36] I. M. Lifshitz and A. M. Kosevich, Sov. Phys. JETP **2**, 639 (1953).
[37] Details of the calculations will be published elsewhere. They are based conceptually on the approach described in a review article in Ref. 18 and very similar to that developed in Ref. 35 for the dHvA oscillations in a MB chain of closed orbits.
[38] P. G. de Gennes, *Superconductivity in Metals and Alloys* (Benjamin, New York, 1966).
[39] T. Champel and V. P. Mineev, Philos. Mag. B **81**, 55 (2001).
[40] V. M. Gvozdikov, Sov. Phys. Solid State **26**, 1560 (1984); **28**, 179 (1986).
[41] V. M. Gvozdikov and M. V. Gvozdikova, Phys. Rev. B **58**, 8716 (1998).
[42] A. A. Slutskin and S. A. Sokolov, JETP Lett. **14**, 60 (1971).
[43] E. Balthes, Ph.D. thesis, Universität Stuttgart, 1997.
[44] L. H. Nguyen, Ph.D. thesis, Hartung-Gorre Verlag Konstanz, 1998.
[45] C. Albrecht, J. H. Smet, D. Weiss, K. von Klitzing, R. Henning, M. Lagenbuch, M. Suhrke, U. Rossler, V. Umansky, and H. Schweizer, Phys. Rev. Lett. **83**, 2234 (1999).
[46] P. D. Grigoriev, M. V. Kartsovnik, W. Biberacher, N. D. Kushch, and P. Wyder, Phys. Rev. B **65**, 060403 (2002).
[47] P. D. Grigoriev, M. V. Kartsovnik, W. Biberacher, and P. Wyder, cond-mat/0108352 (unpublished).